Supporting Information

A Dual-Functional Fibrous Skeleton Implanted with Single-Atomic Co-N_x Dispersions for Longevous Li–S Full Batteries

Ting Huang[1,2,3], Yingjie Sun[4], Jianghua Wu[5], Jia Jin[2], Chaohui Wei[2], Zixiong Shi[2], Menglei Wang[2], Jingsheng Cai[2], Xing-Tao An[4], Peng Wang[5], Chenliang Su[3], Ya-yun Li[1]*, and Jingyu Sun[2]*

[1]College of Materials Science and Engineering, Shenzhen Key Laboratory of Special Functional Materials & Shenzhen Engineering Laboratory for Advance Technology of Ceramics, Shenzhen University, Shenzhen 518060, P. R. China

[2]College of Energy, Soochow Institute for Energy and Materials Innovations (SIEMIS), Jiangsu Provincial Key Laboratory for Advanced Carbon Materials and Wearable Energy Technologies, Soochow University, Suzhou 215006, P. R. China

[3]Institute of Microscale Optoelectronics, International Collaborative Laboratory of 2D Materials for Optoelectronic Science & Technology of Ministry of Education, Shenzhen University, Shenzhen 518060, P. R. China

[4]College of Science, Hebei University of Science and Technology, Shijiazhuang 050018, P. R. China

[5] College of Engineering and Applied Sciences and Collaborative Innovation Center of Advanced Microstructures, National Laboratory of Solid-State Microstructures, Jiangsu Key Laboratory of Artificial Functional Materials, Nanjing University, Nanjing 210093, P. R. China

*Corresponding authors: sunjy86@suda.edu.cn (J. Y. Sun); kittyli@szu.edu.cn (Y.-Y. Li)

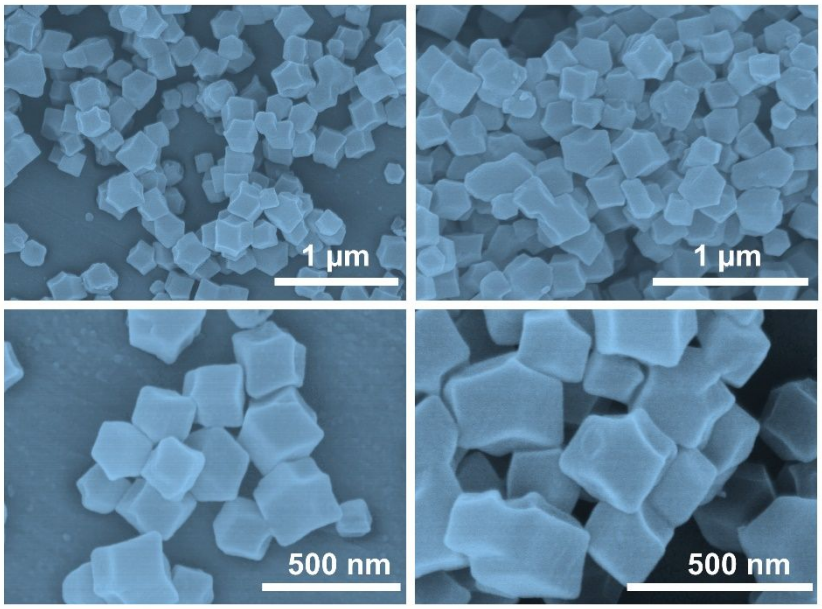

Figure S1. SEM images of as-obtained Co-ZIF8 polyhedrons.

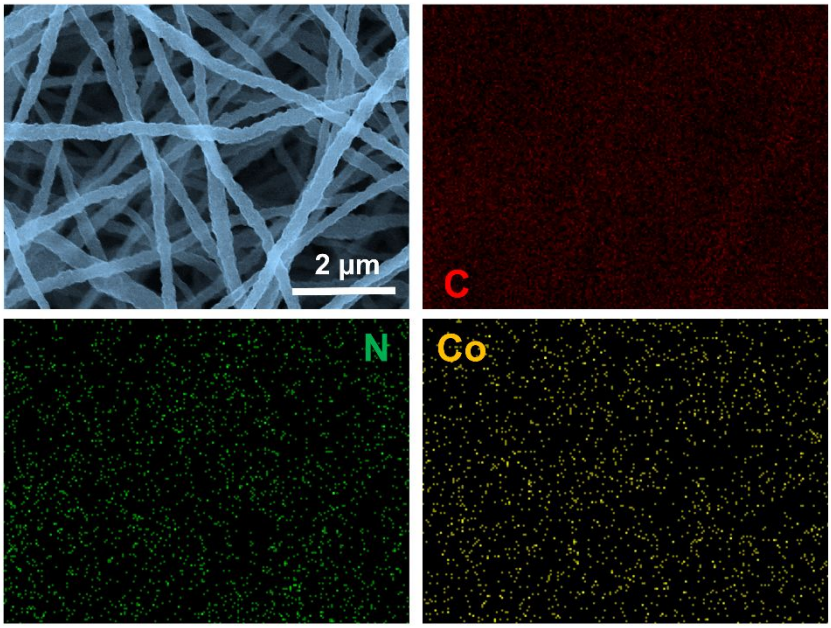

Figure S2. SEM image and corresponding elemental maps of Co-PCNF.

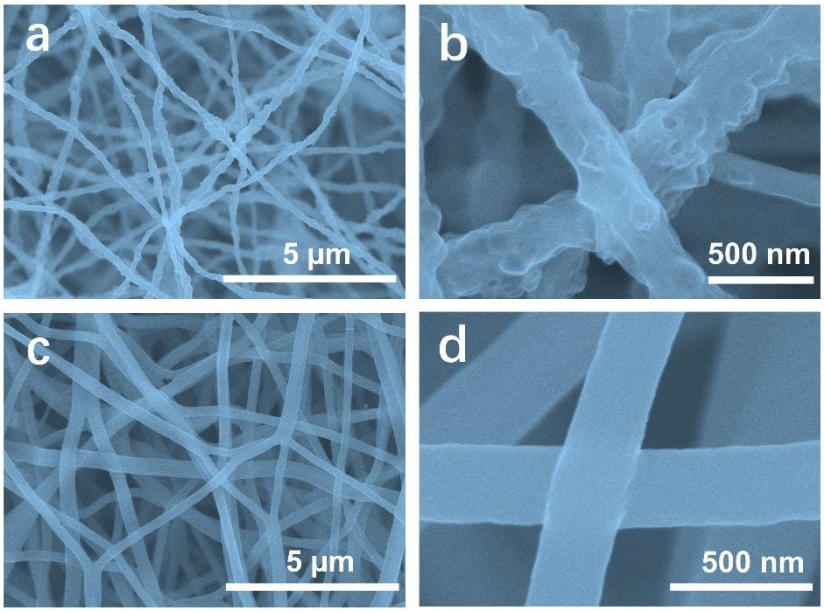

Figure S3. SEM images of (a,b) PCNF and (c,d) CNF.

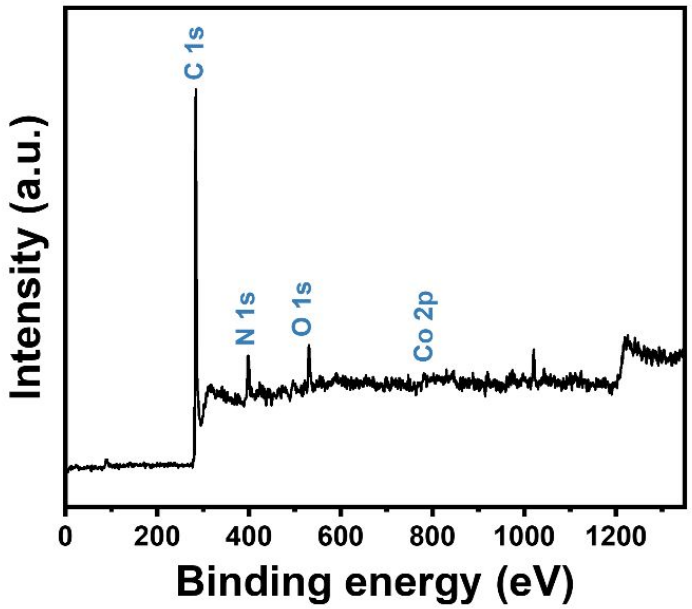

Figure S4. XPS survey spectrum of as-prepared Co-PCNF.

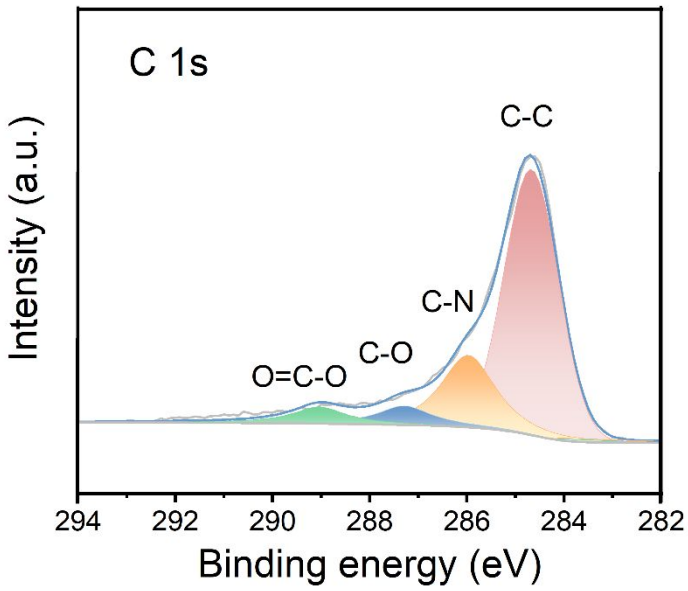

Figure S5. High-resolution XPS C 1s spectrum of Co-PCNF.

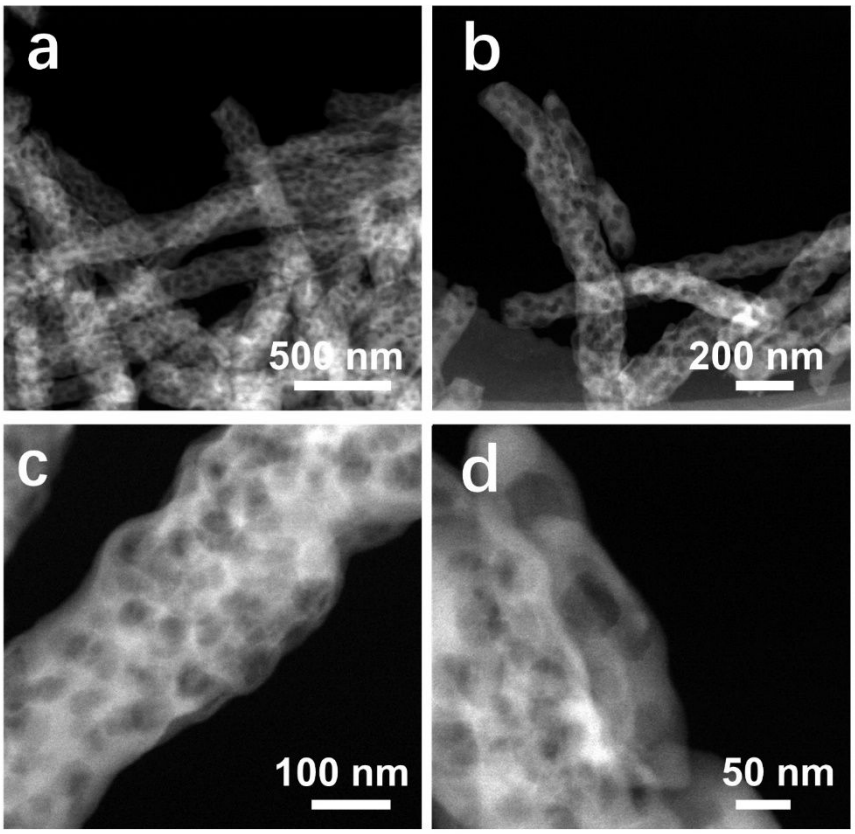

Figure S6. HAADF-STEM images of Co-PCNF.

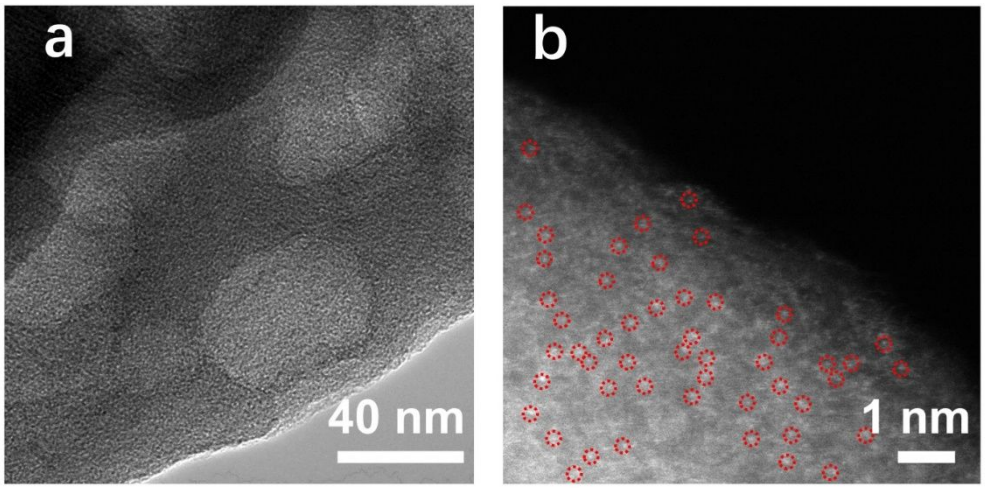

Figure S7. (a) TEM image of Co-PCNF. (b) AC-HAADF-STEM image of Co-PCNF.

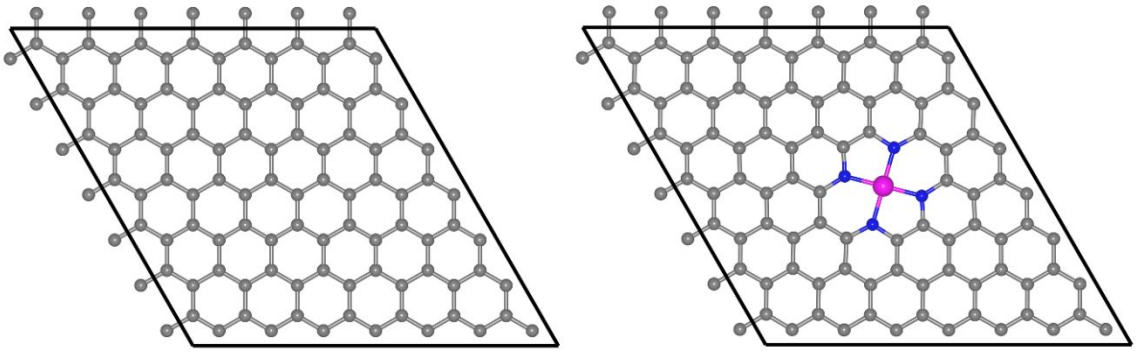

Figure S8. CNF (left panel) and Co-PCNF (right panel) models used in DFT calculations.

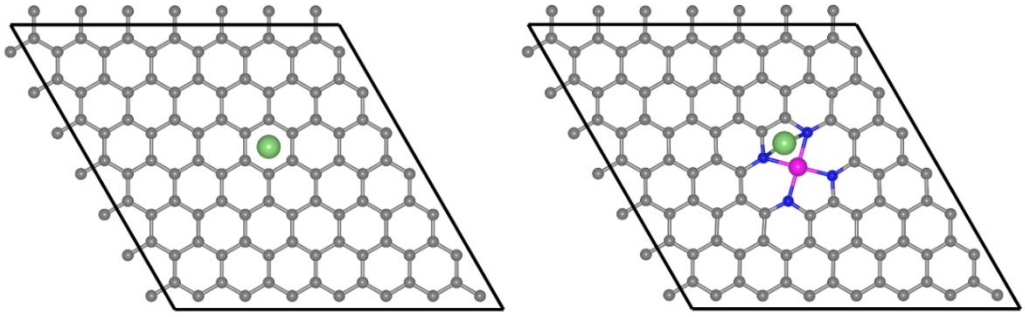

Figure S9. The optimized adsorption configurations of Li atoms on CNF (left panel) and Co-PCNF (right panel).

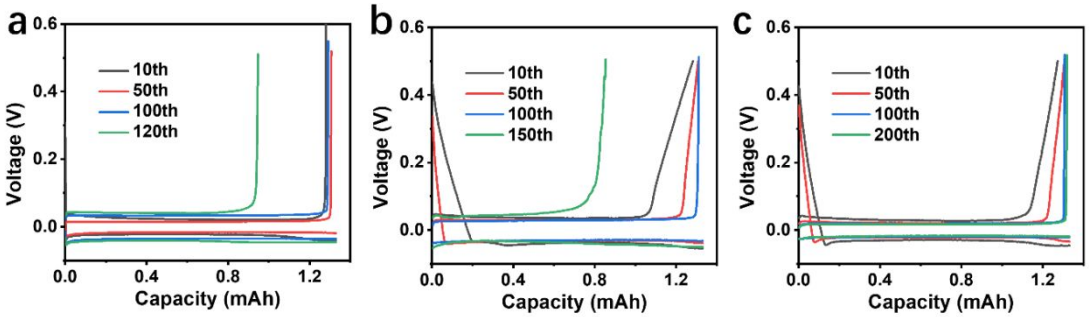

Figure S10. Voltage-capacity curves of (a) Cu foil, (b) PCNF and (c) Co-PCNF at different cycles.

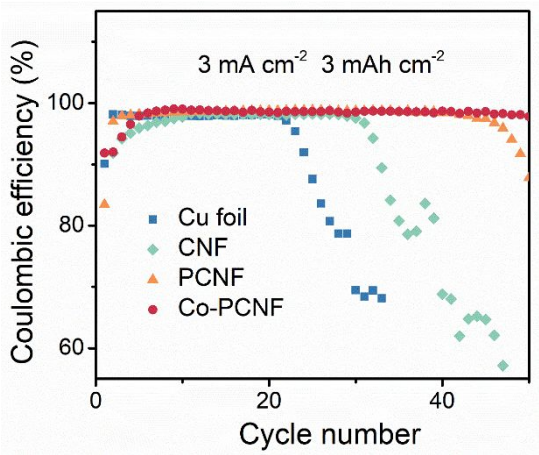

Figure S11. Coulombic efficiencies of different substrates at a current density of 3.0 mA cm^{-2} under a capacity of 3.0 mAh cm^{-2}.

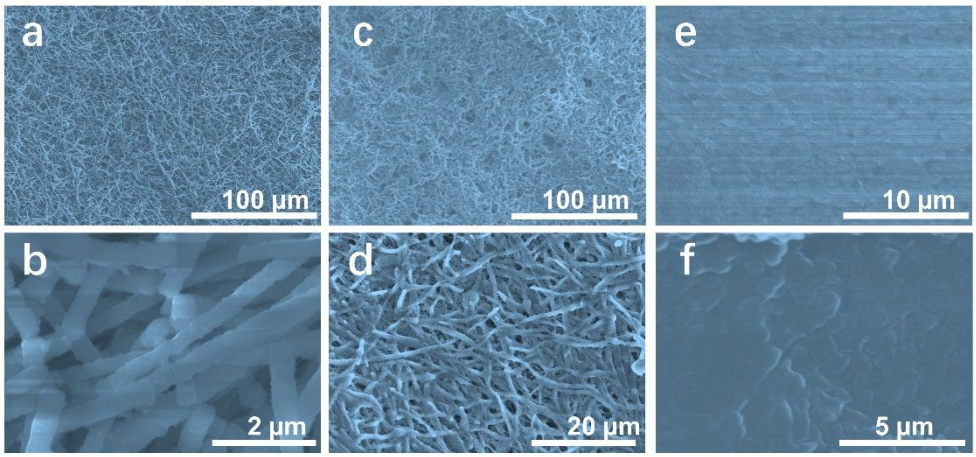

Figure S12. Post-mortem SEM images of the Co-PCNF electrodes with different capacities of Li plating: (a,b) 0.5 mAh cm^{-2}; (c,d) 1.0 mAh cm^{-2}; (e,f) 5.0 mAh cm^{-2}.

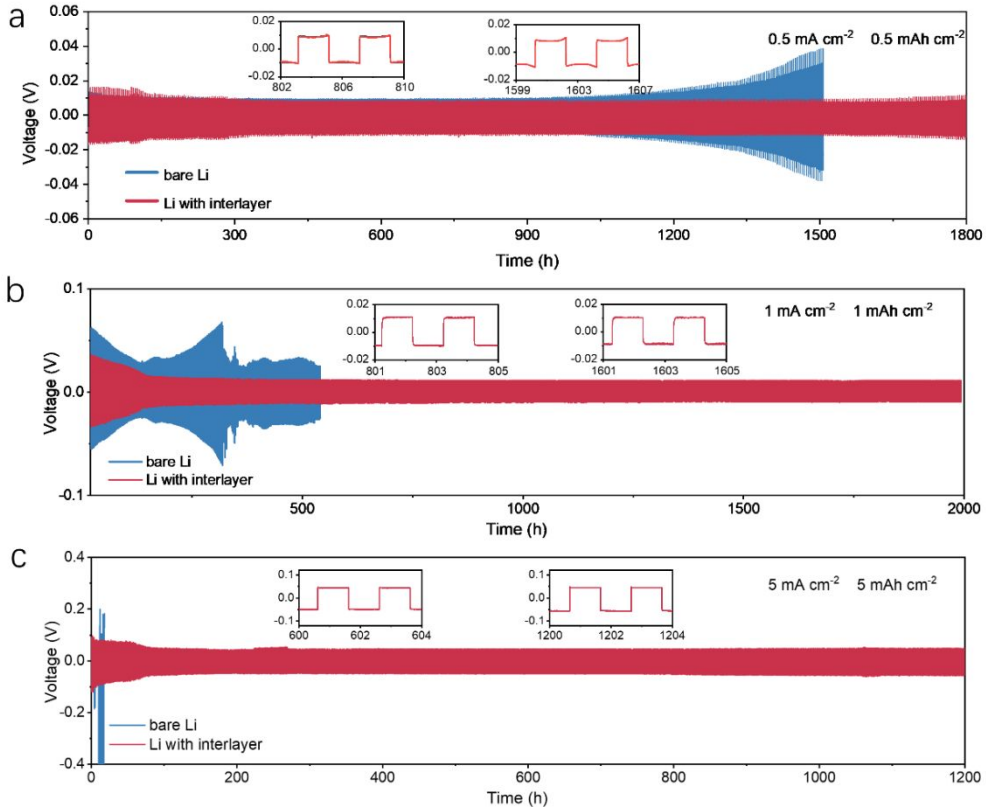

Figure S13. Voltage-time profiles of Li plating/stripping for bare Li and Co-PCNF/Li symmetric cells at different capacities and current densities.

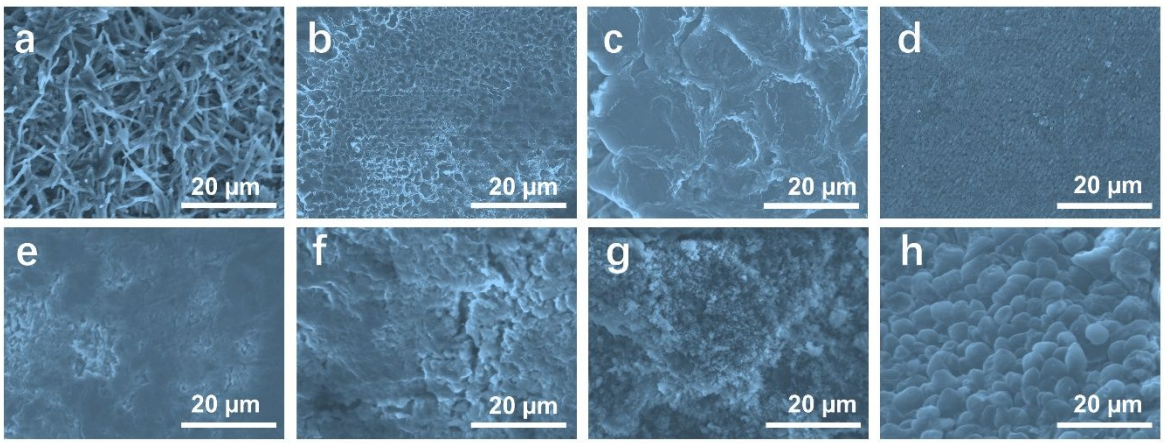

Figure S14. *Ex situ* SEM observations of the morphology evolution for (a-d) Co-PCNF/Li symmetric cell and (e-h) bare Li symmetric cell at a cycling time of (a,e) 10 h; (b,f) 100 h; (c,g) 200 h; (d,h) 400 h.

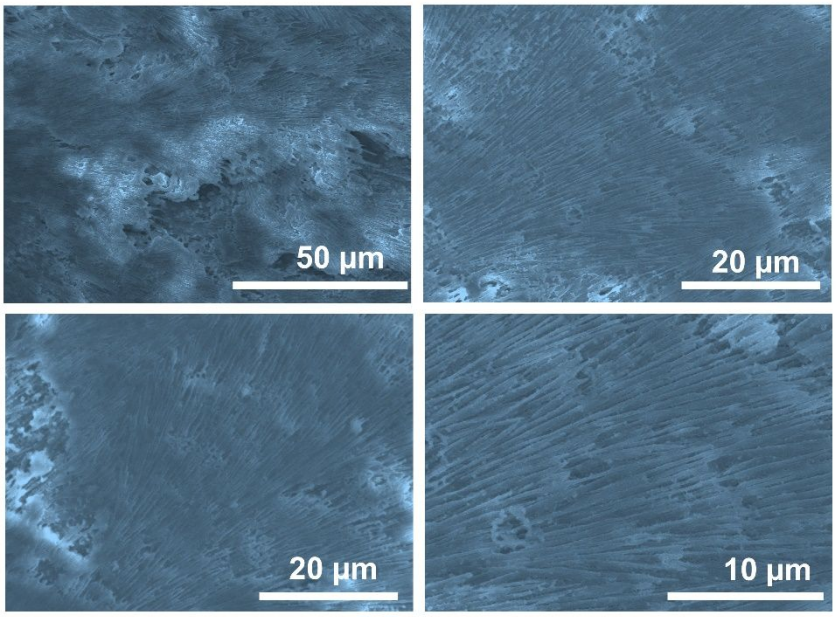

Figure S15. SEM images of Co-PCNF matrix loaded with sulfur.

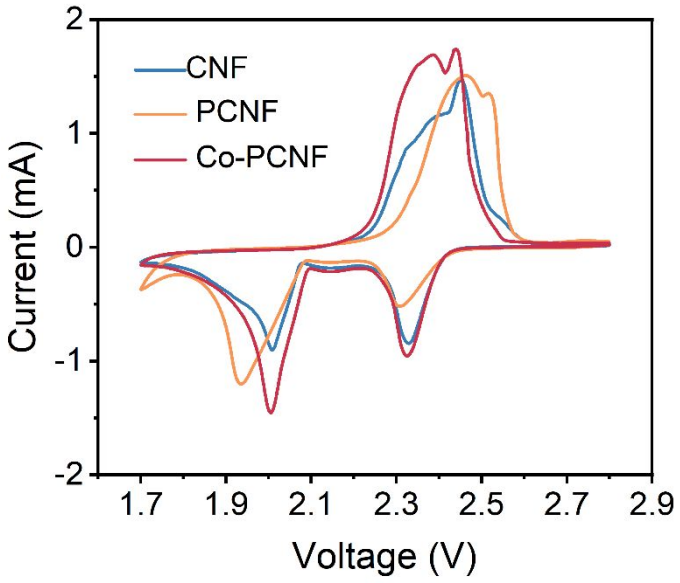

Figure S16. CV curves of S/Co-PCNF, S/PCNF and S/CNF cathodes at a scan rate of 0.05 mV s^{-1}.

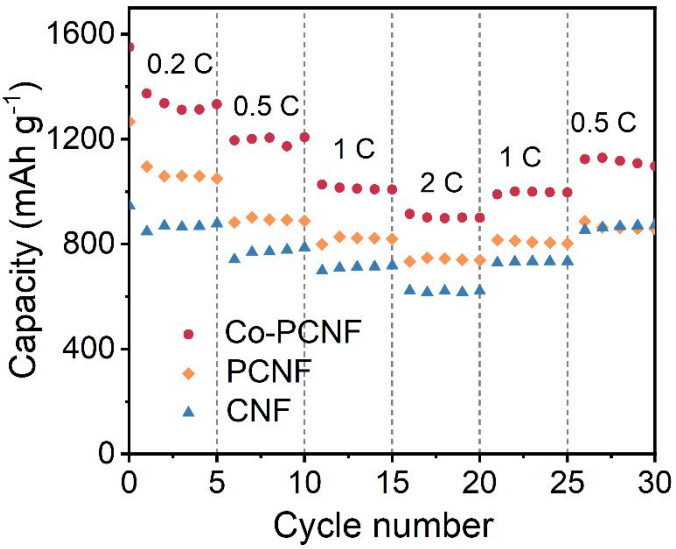

Figure S17. Rate performances of S/Co-PCNF, S/PCNF and S/CNF cathodes.

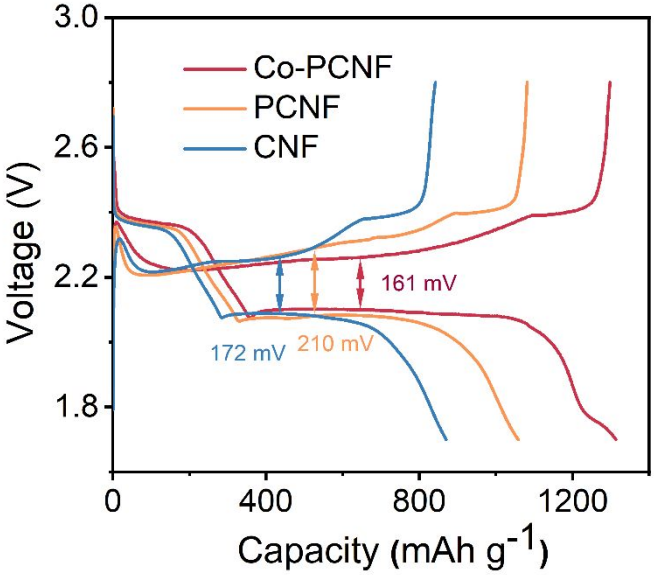

Figure S18. GCD curves of S/Co-PCNF, S/PCNF and S/CNF cathodes at 0.2 C.

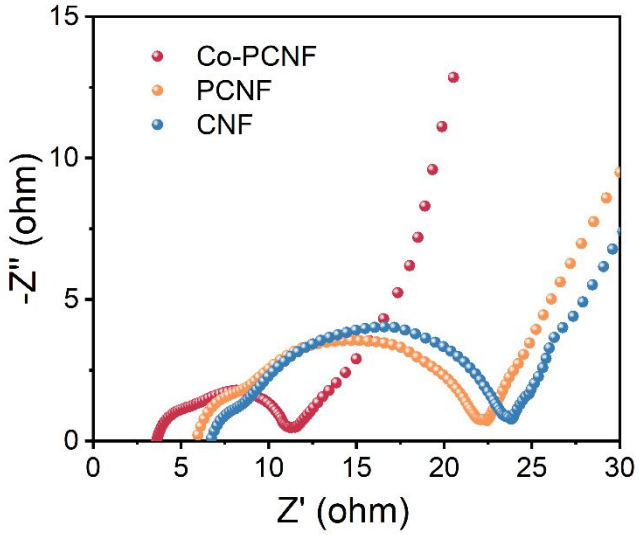

Figure S19. EIS profiles of S/Co-PCNF, S/PCNF and S/CNF cathodes.

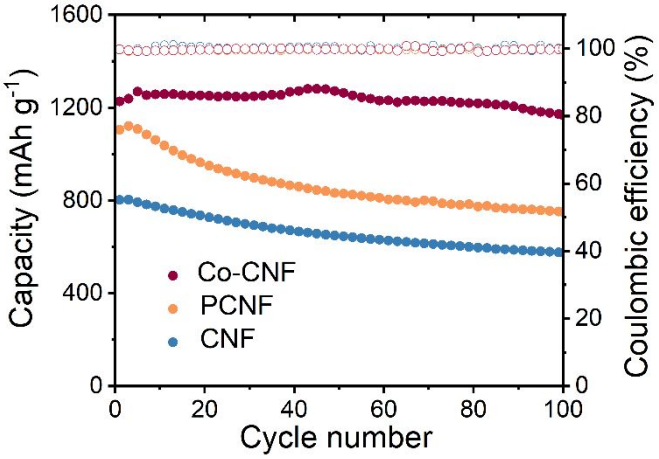

Figure S20. Cycling performances of S/Co-PCNF, S/PCNF and S/CNF cathodes at 0.5 C.

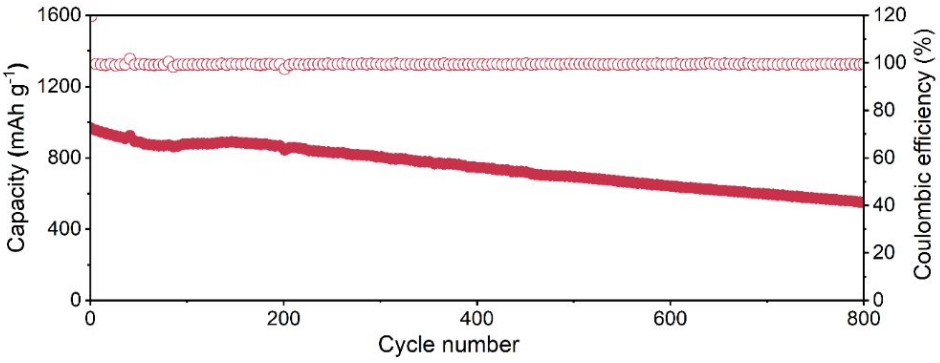

Figure S21. Cycling performance of S/Co-PCNF cathode at 1.0 C.

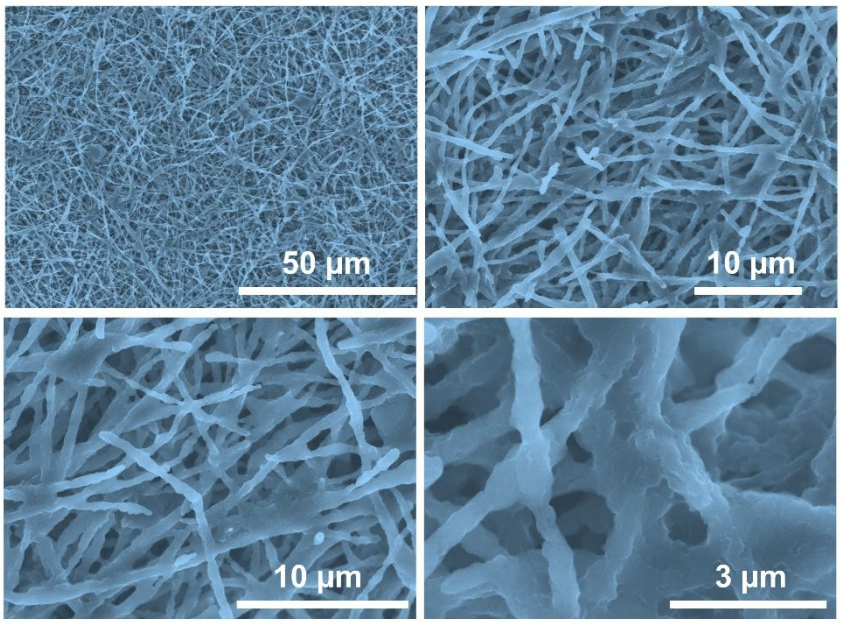

Figure S22. Post-mortem SEM images of S/Co-PCNF cathode at 1.0 C after 800 cycles.

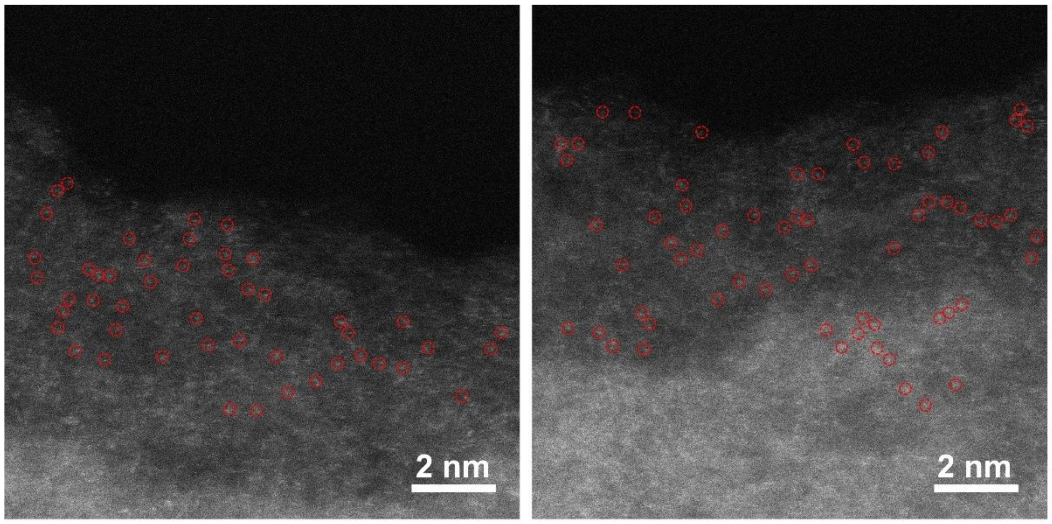

Figure S23. Atomic-resolution HAADF-STEM images of the cycled Co-PCNF after 100 cycles at 0.5 C, showing the preservation of single atoms.

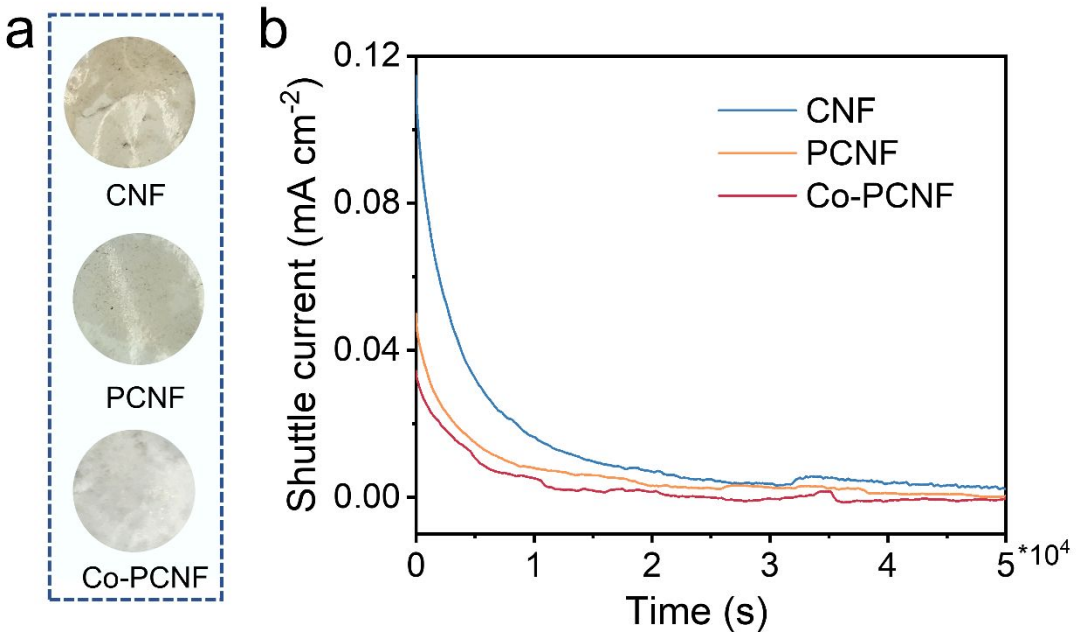

Figure S24. (a) Photographs of the separators of the S/Co-PCNF, S/PCNF and S/CNF paired cells after 100 cycles at 0.5 C; (b) Shuttle current curves of Li–S batteries with S/Co-PCNF, S/PCNF and S/CNF cathodes.

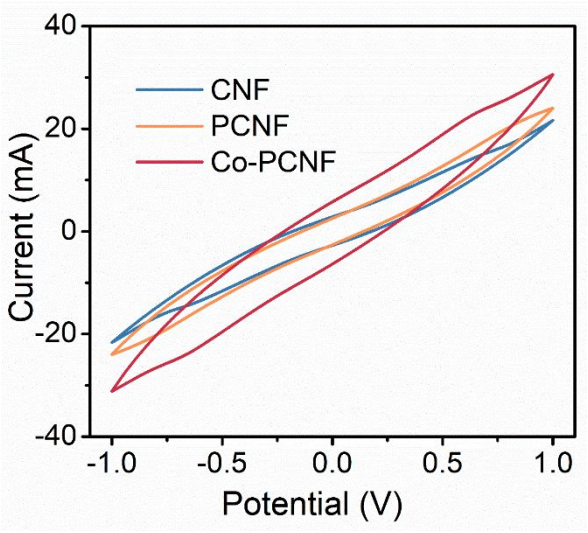

Figure S25. CV profiles of symmetric cells of Co-PCNF, PCNF and CNF at a scan rate of 50 mV s^{-1}.

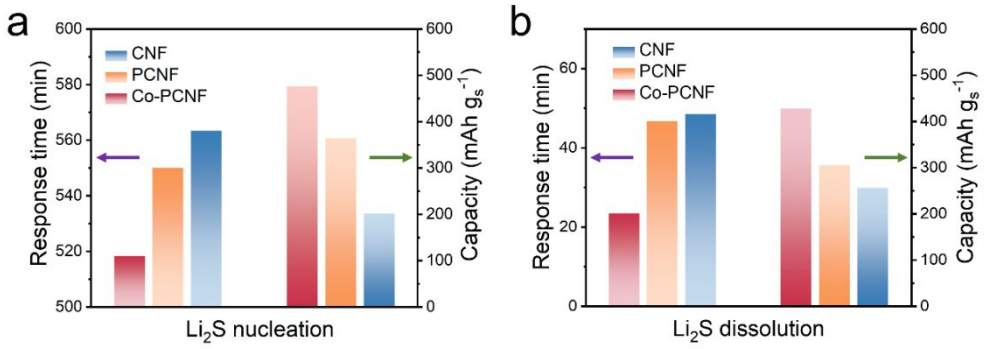

Figure S26. Response time and calculated specific capacity during Li_2S nucleation and dissolution of CNF, PCNF and Co-PCNF paired cells.

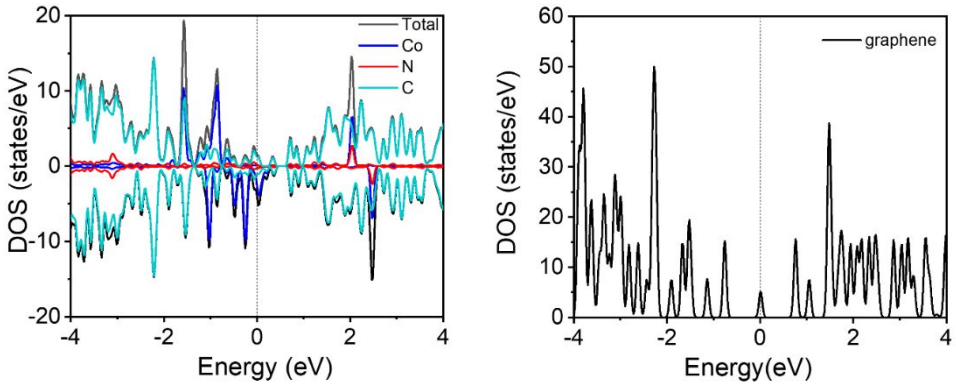

Figure S27. pDOS spectra of Co-PCNF and CNF monolayer.

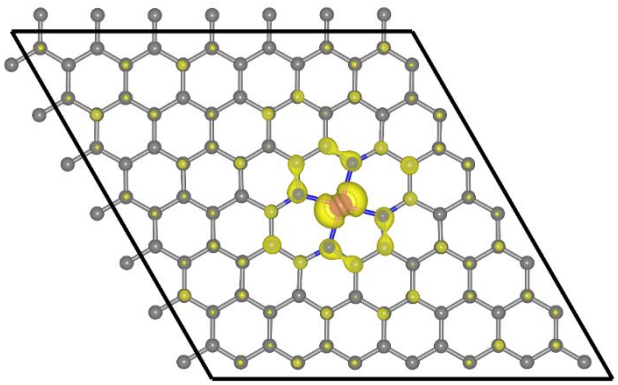

Figure S28. Partial charge density around the Fermi level.

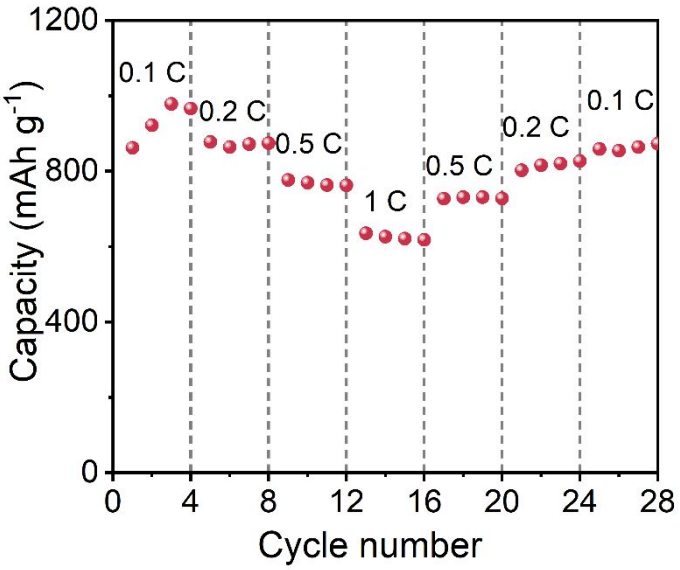

Figure S29. Rate performance of full battery with a sulfur loading of 3.5 mg cm^{-2}.

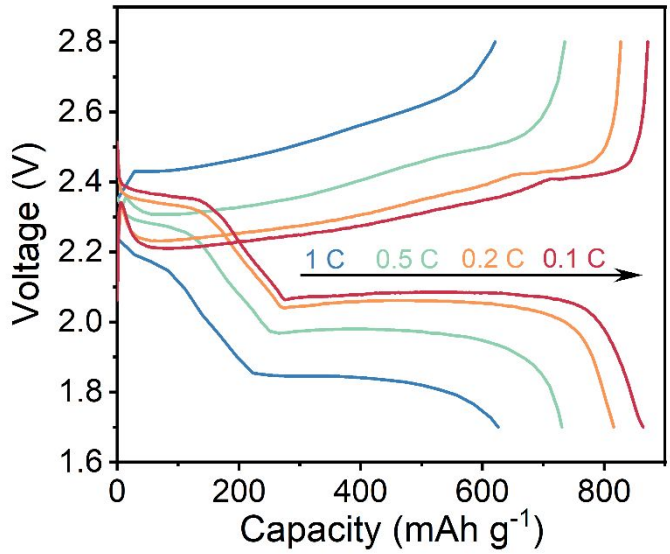

Figure S30. GCD curves of full battery at different current densities.

Table S1. Comparison of single-atom based sulfur hosts between this work and reported studies.

Materials	Sulfur loading	Rate capability	Rate/cycles/capacity retention	Ref
S-SAV@NG	2 mg cm^{-2}	1230 mAh g^{-1} (0.2 C)/645 mAh g^{-1} (3 C)	0.5 C/400/70.64%	[1]
Co-SAs@NC	2 mg cm^{-2}	1425 mAh g^{-1} (0.1 C)/680 mAh g^{-1} (10 C)	1 C/600/72%	[2]
S@Co-N/G	2 mg cm^{-2}	1210 mAh g^{-1} (0.2 C)/618 mAh g^{-1} (4 C)	1 C/500/71.6%	[3]
HFeNG-S	3 mg cm^{-2}	1298 mAh g^{-1} (0.2 C)/810 mAh g^{-1} (5 C)	3 C/600/85.7%	[4]
S-Ni@NG	1.5 mg cm^{-2}	1598 mAh g^{-1} (0.1 C)/612 mAh g^{-1} (10 C)	1 C/500/78%	[5]
Fe-PNC	1.3 mg cm^{-2}	1138.6 mAh g^{-1} (0.1 C)/280 mAh g^{-1} (2 C)	0.5 C/300/80.5%	[6]
Li2S@NC:SAFe	2.0-2.3 mg cm^{-2}	989 mAh g^{-1} (0.5 C)/589 mAh g^{-1} (12 C)	2 C/1000/54.3%	[7]
SC-Co	1.2 mg cm^{-2}	1130 mAh g^{-1} at 0.5 C	0.5 C/300/74.1%	[8]
CoSA-N-C	-	1574 mAh g^{-1} (0.05 C)/624 mAh g^{-1} (5 C)	1 C/1000/65%	[9]
NC@SA-Co	1.0 mg cm^{-2}	-	0.1 C/700/59.4%	[10]
Fe/C_2N	1 mg cm^{-2}	1480 mAh g^{-1} (0.1 C)/683 mAh g^{-1}(5 C)	1 C/900/75.14%	[11]
CNT@SACo	1 mg cm^{-2}	1496 mAh g^{-1}(0.1 C)/641 mAh g^{-1} (2 C)	1 C/500/67.6%	[12]
$Mo{-}N_2/C$	2 mg cm^{-2}	1360.2 mAh g^{-1} (0.1 C)/ 743.9 mAh g^{-1} (5 C)	2 C/550/90.1%	[13]
$Fe\text{-}N_2/CN$	1.3− 1.5 mg cm^{-2}	1301 mAh g^{-1} (0.2 C)/ 607 mAh g^{-1} (5 C)	2 C/2000/78%	[14]
Fe–N/MHCS	2 mg cm^{-2}	1110 mAh g^{-1} (0.2 C)/ 949 mAh g^{-1} (2 C)	0.1 C/200/69.2%	[15]
SA-ZnMXene	1.7 mg cm^{-2}	1136 mAh g^{-1} (0.2 C)/ 517 mAh g^{-1} (6 C)	4 C/400/88%	[16]
Mn/C-(N, O)	1.3 mg cm^{-2}	1330 mAh g^{-1}(0.2 C)/900 mAh g^{-1} (1 C)	0.5 C/600/52%	[17]
Co-PCNF	**1.7 mg cm^{-2}**	**1373.5 mAh g^{-1}(0.2 C)/ 914.3 mAh g^{-1} (2 C)**	**1 C/800/57%**	**This work**

Table S2. Comparison of device performances of Li–S batteries employing "two-in-one" hosts.

Materials	**Curent density (mA cm^{-2}), capacity (mAh cm^{-2})**	**Anode cycle length (h)**	**Sulfur loading (mg cm^{-2})**	**Rate (C)**	**Cycle number**	**Areal capacity (mAh cm^{-2})**	**Ref.**
Co/N-PCNSs	0.5,0.5	350	0.8-1.0	0.2	60	-	[18]
Cu/Ni CF	1,2	500	3.2	~0.4	260	2.4	[19]
VN	2,2	1200	4.0	0.5	~400	4.8	[20]
TiN-VN	2,1	1000	5.6	0.1	100	5.5	[21]
CoNi@PNCFs	1,2	1000	7.0	0.2	50	5.8	[22]
V_8C_7-VO_2	3,1	400	9.2	0.1	100	7.3	[23]
Co-PCNF	**3,3**	**1400**	**6.9**	**0.1**	**50**	**7.1**	**This work**

Table S3. Comparison of electrochemical performances of Li anode employing selected conductive materials.

	Materials	**Curent density (mA cm^{-2}), capacity (mAh cm^{-2})**	**Life span**	**Overpotential**	**Ref**
Carbon cloth (CC)	CC	4, 4	350 h	18 mV	[24]
	Zn@NC@CC	3, 1	400 h	9.6 mV	[25]
	CC@CN-Co	5, 5	1000 h	20 mV	[26]
	N,*P*-codoped CC (NPCC)	5, 1	240 h	140 mV	[27]
	Au-CC	3, 1	350 h	40 mV	[28]
	CC/Co_3O_4-NC	1, 1	1000 h	18 mV	[29]
	NRA-CC	2, 4	1000 h	35 mV	[30]
	CC@ZnO	0.5, 1	1500 h	42 mV	[31]

CNF	3D hollow carbon fiber (3D-HCF)	2, 1	600 h	20 mV	[32]
	CNF/Ag	1, 1	400 h	6.5 mV	[33]
	Ag–CNFs	0.5, 1	500 h	25 mV	[34]
	CFs@Au	1, 2	750 h	60 mV	[35]
	F-rich macroporous CNFs	3, 3	400 h	50 mV	[36]
	NCH@CFs	3, 3	500 h	23 mV	[37]
	Co/CNFs interlayers	0.5, 0.5	1500 h	38.1 mV	[38]
	CNF/TiN	1, 1	600 h	14.1 mV	[39]
Graphene	MnO_2/graphene foam	2, 1	300 h	96 mV	[40]
	rGO	3, 1	70 h	80 mV	[41]
	Ag/GO	40, 1	50 h	120 mV	[42]
	crumpled graphene ball	0.5, 1	750 h	-	[43]
	Au-GA	4, 4	1200 h	87 mV	[44]
	3D rGO Foam	1, 1	500 h	31.2 mV	[45]
	3D *N*-doped graphene	1, 1	1400 h	15 mV	[46]
	G/Li	5, 2.5	1000	-	[47]
Cu nanowire	CuNW network	1, 2	550 h	40 mV	[48]
	Cu-CNF	3, 3	400 h	20 mV	[49]
	CuNW-P	1, 1	1000 h	18 mV	[50]
Cu foam	3D Cu@Ag 3D foam host	2, 2	300h	6.5 mV	[51]
	3D Porous Cu	1, 0.2	1000h	-	[52]
	Cu mesh/Li	2, 1	120 h	-	[53]
	3D HPC/CF	0.5, 1	600 h	27 mV	[54]
	porous Cu current collector porous Cu	1, 1	200 h	20 mV	[55]
	3D Cu_2S NWs/Cu foam	1, 1	140 h	20 mV	[56]
	3D Cu	0.2, 0.5	600 h	50 mV	[57]
	CuO-Cu mesh	5, 1	1000 h	100 mV	[58]
Ni foam	Ni foam	1, 5	40 h	200 mV	[59]
	3D porous Ni	1,1	600 h	-	[60]
	$NiCo_2O_4$@ Ni foam	1, 1	1000 h	16 mV	[61]

	V_2O_5@ Ni foam	1, 1	1600 h	18 mV	[62]
	ZnO@ Ni foam	5, 1	250 cycles	45 mV	[63]
	Ni_2P@nickel foam	2, 1	2000 h	-	[64]
	Ni_3N@ nickel foam	5, 1	160 cycles	34 mV	[65]
	NCNT/NF	3, 3	400 h	62 mV	[66]
	Co-PCNF	**5, 5**	**1200 h**	**40 mV**	**This work**

Table S4. Comparison of electrochemical performances of sulfur cathode employing selected conductive materials.

	Material	**Sulfur loading**	**Rate capability**	**Rate/cycles/capacity decay per cycle**	**Ref**
Carbon cloth (CC)	CoP@G/CC	2 mg cm^{-2}	1371.9 mAh g^{-1} (0.2 C)/ 930.1 mAh g^{-1} (3 C)	2C/500/0.03%	[67]
	VSe_2−VG@ CC	1.4−1.7 mg cm^{-2}	1480 mAh g^{-1} (0.2 C)/ 450 mAh g^{-1} (5.0 C)	5 C/800/0.039%	[68]
	CC@WS_2	1.0−1.2 mg cm^{-2}	1581 mAh g^{-1} (0.1 C)/ 448 mA h g^{-1} (3 C)	0.5 C/500/0.0313%	[69]
	CC-CoS_2	1.2 mg cm^{-2}	1481 mAh g^{-1}(0.1 C)/ 823 mAh g^{-1}(4 C)	4C/1000/0.021%	[70]
	ZnS_{1-x}/CC	1.7 mg cm^{-2}	1043 mAh g^{-1} (0.2 C)/ 374 mAh g^{-1}(5 C)	1 C/500/0.04%	[71]
	CC@CoP/C	1.81 mg cm^{-2}	1201 mAh g^{-1}(0.1 C)/ 708 mA h g^{-1}(2 C)	2C/600/0.016%	[72]
	CC@SnO_2 @TMS	2.75 mg cm^{-2}	1500 mAh g^{-1} (0.2 C)/ 860 mAh g^{-1}(5 C)	5 C/4000/0.009%	[73]
	CC/VN	8.1 mg cm^{-2}	1310.8 mAh g^{-1} (0.1 C)/ 591.6 mAh g^{-1} (5 C)	0.1C/250/0.078%	[74]
Carbon nanotube (CNT)	CNT paper	2.0 mg cm^{-2}	1093 mAh g^{-1}(0.38 mA cm^{-2})/ 814 mA·h g^{-1}(1.51 mA cm^{-2})	0.05 C/150/0.2%	[75]
	CNT-UGF	2.4 mg cm^{-2}	-	0.5 C/400/0.063%	[76]
	HKUST-1/CNT	1mg cm^{-2}	1,263 mAh g^{-1} at (0.2 C)/449 mAh g^{-1} (10 C)	0.2 C/500/0.08%	[77]
	porous CNT microspheres	~2.0 mg cm^{-2}	1200 mAh g^{-1}(0.2 C)/785 mAh g^{-1}(3.0 C)	1 C/500/0.046%	[78]
	CNT@MPC	1 mg cm^{-2}	1200 mAh g^{-1} (0.1 C)/800	0.1 C/200/0.05%	[79]

			mAh g^{-1} (5 C)		
	CNTs/Co_3S_4–NBs	1.2 mg cm^{-2}	1330 mAh g^{-1} (0.2 C)/ 702 mAh g^{-1} (5 C)	1 C/500/0.042%	[80]
	CoP-CNT	3 mg cm^{-2}	-	1 C/200/0.018%	[81]
	Macropore CNT particles (M-CNTPs)	1 mg cm^{-2}	1343 mA h g^{-1}(0.2 C)/ 992 mA h g^{-1} (2 C)	2 C/100/0.29%	[82]
Carbon nanofiber (CNF)	nitrogen-doped porous carbon nanofibers (NPCN)	6.1 mg cm^{-2}	1248 mA h g^{-1} (0.05 C)/ 702 mA h g^{-1} (2 C)	0.5 C/400/0.04%	[83]
	CPZC	1.5 mg cm^{-2}	1200 mAh g^{-1}(0.2 C)/622.6 mAh g^{-1} (10 C)	1 C/2000/0.016%	[84]
	porous CNFs	2.0 mg	954 mAh g^{-1} (0.5 C)/ 602.2 mAh g^{-1}(2 C)	0.5 C/350/ 0.068%	[85]
	activated multichannel CNF	2.2 mg cm^{-2}	1351 mAh g^{-1} (0.2 C)/ 847 mA h g^{-1} (5 C)	0.2 C/300/0.07%	[86]
	activated PCNT	2.2 mg cm^{-2}	1270 mAh g^{-1}(0.2 C)/ 857 mAh g^{-1} (5 C)	0.2 C/300/0.09%	[87]
	LRC/S@EFG	3.6 mg cm^{-2}	1,300 mAh g^{-1}(0.1 C)/ 363 mAh g^{-1} (2 C)	0.2 C/200/0.1%	[88]
	CNF@Co_3S_4	1.7 mg cm^{-2}	1079 mA h g^{-1}(0.1 C)/ 850 mA h g^{-1}(1.5 C)	1 C/200/0	[89]
	GC-TiO@CHF	5 mg cm^{-2}	1,000 mAh g^{-1} (0.1 C)/ 620 mAh g^{-1}(2 C)	0.2 C/400/0.085%	[90]
Graphene	*N*-doped graphene sheet	1.5 mg cm^{-2}	1486 mAh g^{-1}(0.1 C)/ 950 mAh g^{-1}(1 C)	1.17 mA cm^{-2}/300/ 0.08%	[91]
	rNGO	1.2 mg cm^{-2}	803 mAh g^{-1}(0.1 C)/ 592 mAh g^{-1}(1 C)	1C/1000/-	[92]
	hydrothermally reduced graphene oxide (HrGO)	1.3-1.6 mg cm^{-2}	1033 mAh g^{-1}(0.1 C)/ 588 mAh g^{-1} (1 C)	1.5 A g^{-1}/ 500 / 0.07%	[93]
	3D *N*-doped graphene foam	2.05 mg cm^{-2}	1145 mAh g^{-1} (0.1 C)/ 625 mAh g^{-1} (2 C)	2 C/500/0.061%	[94]
	GA composite	2.5 mg cm^{-2}	1100 mAh g^{-1}(0.1 C)/300 mAh g^{-1} (1 C)	0.5 C/200/-	[95]

	hierarchical porous graphene	-	1068 mAh g^{-1} (0.5 C)/ 543 mAh g^{-1} (10 C)	1C/80/-	[96]
	N,*S* co-doped porous graphene matrix	1.5 mg cm^{-2}	1203 mAh g^{-1} (0.1 C)/ 855 mAh g^{-1} (2 C)	0.2 C/600/0.056%	[97]
	rGO	2.2 mg cm^{-2}	1200 mAh g^{-1} (0.1 C)/ 924 mAh g^{-1} (2 C)	0.1 C/200/0.12%	[98]
	Co-PCNF	**1.7 mg cm^{-2}**	**1373.5 mAh g^{-1}(0.2 C)/ 914.3 mAh g^{-1} (2.0 C)**	**1 C/800/0.05%**	**This work**

REFERENCES

1. Zhou, G.; Zhao, S.; Wang, T.; Yang, S. Z.; Johannessen, B.; Chen, H.; Liu, C.; Ye, Y.; Wu, Y.; Peng, Y.; Liu, C.; Jiang, S. P.; Zhang, Q.; Cui, Y., Theoretical Calculation Guided Design of Single-Atom Catalysts toward Fast Kinetic and Long-Life Li-S Batteries. *Nano Lett.* **2020,** *20*, 1252-1261.
2. Li, Y.; Chen, G.; Mou, J.; Liu, Y.; Xue, S.; Tan, T.; Zhong, W.; Deng, Q.; Li, T.; Hu, J.; Yang, C.; Huang, K.; Liu, M., Cobalt Single Atoms Supported on *N*-Doped Carbon as An Active and Resilient Sulfur Host for Lithium–Sulfur Batteries. *Energy Storage Mater.* **2020,** *28*, 196-204.
3. Du, Z.; Chen, X.; Hu, W.; Chuang, C.; Xie, S.; Hu, A.; Yan, W.; Kong, X.; Wu, X.; Ji, H.; Wan, L. J., Cobalt in Nitrogen-Doped Graphene as Single-Atom Catalyst for High-Sulfur Content Lithium-Sulfur Batteries. *J. Am. Chem. Soc.* **2019,** *141*, 3977-3985.
4. Wang, Y.; Adekoya, D.; Sun, J.; Tang, T.; Qiu, H.; Xu, L.; Zhang, S.; Hou, Y., Manipulation of Edge-Site Fe–N_2 Moiety on Holey *Fe*, *N* Codoped Graphene to Promote the Cycle Stability and Rate Capacity of Li–S Batteries. *Adv. Funct. Mater.* **2019,** *29*, 1807485.
5. Zhang, L.; Liu, D.; Muhammad, Z.; Wan, F.; Xie, W.; Wang, Y.; Song, L.; Niu, Z.; Chen, J., Single Nickel Atoms on Nitrogen-Doped Graphene Enabling Enhanced Kinetics of Lithium-Sulfur Batteries. *Adv. Mater.* **2019,** *31*, 1903955.
6. Liu, Z.; Zhou, L.; Ge, Q.; Chen, R.; Ni, M.; Utetiwabo, W.; Zhang, X.; Yang, W., Atomic Iron Catalysis of Polysulfide Conversion in Lithium-Sulfur Batteries. *ACS Appl. Mater. Interfaces* **2018,** *10*, 19311-19317.
7. Wang, J.; Jia, L.; Zhong, J.; Xiao, Q.; Wang, C.; Zang, K.; Liu, H.; Zheng, H.; Luo, J.; Yang, J.; Fan, H.; Duan, W.; Wu, Y.; Lin, H.; Zhang, Y., Single-Atom Catalyst Boosts Electrochemical Conversion Reactions in Batteries. *Energy Storage Mater.* **2019,** *18*, 246-252.
8. Xie, J.; Li, B. Q.; Peng, H. J.; Song, Y. W.; Zhao, M.; Chen, X.; Zhang, Q.; Huang, J. Q., Implanting Atomic Cobalt within Mesoporous Carbon toward Highly Stable Lithium-Sulfur Batteries. *Adv. Mater.* **2019,** *31*, 1903813.
9. Li, Y.; Wu, J.; Zhang, B.; Wang, W.; Zhang, G.; Seh, Z. W.; Zhang, N.; Sun, J.; Huang, L.;

Jiang, J.; Zhou, J.; Sun, Y., Fast Conversion and Controlled Deposition of Lithium (Poly)Sulfides in Lithium-Sulfur Batteries Using High-Loading Cobalt Single Atoms. *Energy Storage Mater.* **2020,** *30*, 250-259.

10. Li, Y.; Zhou, P.; Li, H.; Gao, T.; Zhou, L.; Zhang, Y.; Xiao, N.; Xia, Z.; Wang, L.; Zhang, Q.; Gu, L.; Guo, S., A Freestanding Flexible Single-Atom Cobalt-Based Multifunctional Interlayer toward Reversible and Durable Lithium-Sulfur Batteries. *Small Methods* **2020,** *4*, 1900701.

11. Liang, Z.; Yang, D.; Tang, P.; Zhang, C.; Jacas Biendicho, J.; Zhang, Y.; Llorca, J.; Wang, X.; Li, J.; Heggen, M.; David, J.; Dunin-Borkowski, R. E.; Zhou, Y.; Morante, J. R.; Cabot, A.; Arbiol, J., Atomically Dispersed Fe in a C_2N Based Catalyst as a Sulfur Host for Efficient Lithium–Sulfur Batteries. *Adv. Energy Mater.* **2020,** *11*, 2003507.

12. Lin, Q.; Ding, B.; Chen, S.; Li, P.; Li, Z.; Shi, Y.; Dou, H.; Zhang, X., Atomic Layer Deposition of Single Atomic Cobalt as a Catalytic Interlayer for Lithium–Sulfur Batteries. *ACS Appl. Energy Mater.* **2020,** *3*, 11206-11212.

13. Ma, F.; Wan, Y.; Wang, X.; Wang, X.; Liang, J.; Miao, Z.; Wang, T.; Ma, C.; Lu, G.; Han, J.; Huang, Y.; Li, Q., Bifunctional Atomically Dispersed Mo-N_2/C Nanosheets Boost Lithium Sulfide Deposition/Decomposition for Stable Lithium-Sulfur Batteries. *ACS Nano* **2020,** *14*, 10115-10126.

14. Qiu, Y.; Fan, L.; Wang, M.; Yin, X.; Wu, X.; Sun, X.; Tian, D.; Guan, B.; Tang, D.; Zhang, N., Precise Synthesis of Fe-N_2 Sites with High Activity and Stability for Long-Life Lithium-Sulfur Batteries. *ACS Nano* **2020,** *14*, 16105-16113.

15. Shao, Q.; Xu, L.; Guo, D.; Su, Y.; Chen, J., Atomic Level Design of Single Iron Atom Embedded Mesoporous Hollow Carbon Spheres as Multi-Effect Nanoreactors for Advanced Lithium–Sulfur Batteries. *J. Mater. Chem. A* **2020,** *8*, 23772-23783.

16. Zhang, D.; Wang, S.; Hu, R.; Gu, J.; Cui, Y.; Li, B.; Chen, W.; Liu, C.; Shang, J.; Yang, S., Catalytic Conversion of Polysulfides on Single Atom Zinc Implanted MXene toward High-Rate Lithium–Sulfur Batteries. *Adv. Funct. Mater.* **2020,** *30*, 2002471.

17. Liu, Y.; Wei, Z.; Zhong, B.; Wang, H.; Xia, L.; Zhang, T.; Duan, X.; Jia, D.; Zhou, Y.; Huang, X., O-, N-Coordinated Single Mn Atoms Accelerating Polysulfides Transformation in Lithium-Sulfur Batteries. *Energy Storage Mater.* **2021,** *35*, 12-18.

18. Liu, S.; Li, J.; Yan, X.; Su, Q.; Lu, Y.; Qiu, J.; Wang, Z.; Lin, X.; Huang, J.; Liu, R.; Zheng, B.; Chen, L.; Fu, R.; Wu, D., Superhierarchical Cobalt-Embedded Nitrogen-Doped Porous Carbon Nanosheets as Two-in-One Hosts for High-Performance Lithium-Sulfur Batteries. *Adv. Mater.* **2018,** *30*, 1706895.

19. Chang, J.; Shang, J.; Sun, Y.; Ono, L. K.; Wang, D.; Ma, Z.; Huang, Q.; Chen, D.; Liu, G.; Cui, Y.; Qi, Y.; Zheng, Z., Flexible and Stable High-Energy Lithium-Sulfur Full Batteries with Only 100% Oversized Lithium. *Nat. Commun.* **2018,** *9*, 4480.

20. He, J.; Manthiram, A., Long-Life, High-Rate Lithium–Sulfur Cells with a Carbon-Free VN Host as an Efficient Polysulfide Adsorbent and Lithium Dendrite Inhibitor. *Adv. Energy Mater.* **2019,** *10*, 1903241.

21. Yao, Y.; Wang, H.; Yang, H.; Zeng, S.; Xu, R.; Liu, F.; Shi, P.; Feng, Y.; Wang, K.; Yang, W.; Wu, X.; Luo, W.; Yu, Y., A Dual-Functional Conductive Framework Embedded with TiN-VN Heterostructures for Highly Efficient Polysulfide and Lithium Regulation toward Stable Li-S Full Batteries. *Adv. Mater.* **2020,** *32*, 1905658.

22. He, Y.; Li, M.; Zhang, Y.; Shan, Z.; Zhao, Y.; Li, J.; Liu, G.; Liang, C.; Bakenov, Z.; Li, Q., All-Purpose Electrode Design of Flexible Conductive Scaffold toward High-Performance Li–S

Batteries. *Adv. Funct. Mater.* **2020,** *30*, 2000613.
23. Cai, J.; Jin, J.; Fan, Z.; Li, C.; Shi, Z.; Sun, J.; Liu, Z., 3D Printing of a V_8C_7-VO_2 Bifunctional Scaffold as an Effective Polysulfide Immobilizer and Lithium Stabilizer for Li-S Batteries. *Adv. Mater.* **2020,** *32*, 2005967.
24. Wang, Q.; Yang, C.; Yang, J.; Wu, K.; Qi, L.; Tang, H.; Zhang, Z.; Liu, W.; Zhou, H., Stable Li Metal Anode with Protected Interface for High-Performance Li Metal Batteries. *Energy Storage Mater.* **2018,** *15*, 249-256.
25. You, L.; Ju, S.; Liu, J.; Xia, G.; Guo, Z.; Yu, X., Synergistic Effect of Lithiophilic Zn Nanoparticles and *N*-Doping for Stable Li Metal Anodes. *J. Energy Chem.* **2022,** *65*, 439-447.
26. Zhou, T.; Shen, J.; Wang, Z.; Liu, J.; Hu, R.; Ouyang, L.; Feng, Y.; Liu, H.; Yu, Y.; Zhu, M., Regulating Lithium Nucleation and Deposition *via* MOF-Derived Co@C-Modified Carbon Cloth for Stable Li Metal Anode. *Adv. Funct. Mater.* **2020,** *30* (14), 1909159.
27. Li, K.; Hu, Z.; Ma, J.; Chen, S.; Mu, D.; Zhang, J., A 3D and Stable Lithium Anode for High-Performance Lithium-Iodine Batteries. *Adv. Mater.* **2019,** *31* (33), 1902399.
28. Chen, W.; Fu, M.; Zhao, Q.; Zhou, A.; Huang, W.; Wang, J., Au-Modified 3D Carbon Cloth as a Dendrite-Free Framework for Li Metal with Excellent Electrochemical Stability. *J. Alloys Compd.* **2021,** *871*, 159491.
29. Jiang, G.; Jiang, N.; Zheng, N.; Chen, X.; Mao, J.; Ding, G.; Li, Y.; Sun, F.; Li, Y., MOF-Derived Porous Co_3O_4-NC Nanoflake Arrays on Carbon Fiber Cloth as Stable Hosts for Dendrite-Free Li Metal Anodes. *Energy Storage Mater.* **2019,** *23*, 181-189.
30. Wang, T. S.; Liu, X.; Wang, Y.; Fan, L. Z., High Areal Capacity Dendrite-Free Li Anode Enabled by Metal–Organic Framework-Derived Nanorod Array Modified Carbon Cloth for Solid State Li Metal Batteries. *Adv. Funct. Mater.* **2020,** *31* (2), 2001973.
31. Wang, X.; Pan, Z.; Wu, Y.; Ding, X.; Hong, X.; Xu, G.; Liu, M.; Zhang, Y.; Li, W., Infiltrating Lithium into Carbon Cloth Decorated with Zinc Oxide Arrays for Dendrite-Free Lithium Metal Anode. *Nano Res.* **2018,** *12* (3), 525-529.
32. Liu, L.; Yin, Y.-X.; Li, J.-Y.; Li, N.-W.; Zeng, X.-X.; Ye, H.; Guo, Y.-G.; Wan, L.-J., Free-Standing Hollow Carbon Fibers as High-Capacity Containers for Stable Lithium Metal Anodes. *Joule* **2017,** *1* (3), 563-575.
33. Zhang, R.; Chen, X.; Shen, X.; Zhang, X.-Q.; Chen, X.-R.; Cheng, X.-B.; Yan, C.; Zhao, C.-Z.; Zhang, Q., Coralloid Carbon Fiber-Based Composite Lithium Anode for Robust Lithium Metal Batteries. *Joule* **2018,** *2* (4), 764-777.
34. Yang, C.; Yao, Y.; He, S.; Xie, H.; Hitz, E.; Hu, L., Ultrafine Silver Nanoparticles for Seeded Lithium Deposition toward Stable Lithium Metal Anode. *Adv. Mater.* **2017,** *29* (38), 1702714.
35. Xiang, J.; Yuan, L.; Shen, Y.; Cheng, Z.; Yuan, K.; Guo, Z.; Zhang, Y.; Chen, X.; Huang, Y., Improved Rechargeability of Lithium Metal Anode *via* Controlling Lithium-Ion Flux. *Adv. Energy Mater.* **2018,** *8* (36), 1802352.
36. Zhao, Y.; Chen, B.; Xia, S.; Yu, J.; Yan, J.; Ding, B., Selective Nucleation and Targeted Deposition Effect of Lithium in a Lithium-Metal Host Anode. *J. Mater. Chem. A* **2021,** *9* (9), 5381-5389.
37. Chen, C.; Guan, J.; Li, N. W.; Lu, Y.; Luan, D.; Zhang, C. H.; Cheng, G.; Yu, L.; Lou, X. W. D., Lotus-Root-Like Carbon Fibers Embedded with Ni-Co Nanoparticles for Dendrite-Free Lithium Metal Anodes. *Adv. Mater.* **2021**, 2100608.
38. Shu, M.; Li, X.; Duan, L.; Zhu, M.; Xin, X., Nitrogen-Doped Polymer Nanofibers Decorated

with Co Nanoparticles for Uniform Lithium Nucleation/Growth in Lithium Metal Batteries. *Nanoscale* **2020,** *12* (16), 8819-8827.
39. Lin, K.; Qin, X.; Liu, M.; Xu, X.; Liang, G.; Wu, J.; Kang, F.; Chen, G.; Li, B., Ultrafine Titanium Nitride Sheath Decorated Carbon Nanofiber Network Enabling Stable Lithium Metal Anodes. *Adv. Funct. Mater.* **2019,** *29* (46), 1903229.
40. Yu, B.; Tao, T.; Mateti, S.; Lu, S.; Chen, Y., Nanoflake Arrays of Lithiophilic Metal Oxides for the Ultra-Stable Anodes of Lithium-Metal Batteries. *Adv. Funct. Mater.* **2018,** *28* (36), 1803023.
41. Lin, D.; Liu, Y.; Liang, Z.; Lee, H. W.; Sun, J.; Wang, H.; Yan, K.; Xie, J.; Cui, Y., Layered Reduced Graphene Oxide with Nanoscale Interlayer Gaps as a Stable Host for Lithium Metal Anodes. *Nat. Nanotechnol.* **2016,** *11* (7), 626-32.
42. Xue, P.; Liu, S.; Shi, X.; Sun, C.; Lai, C.; Zhou, Y.; Sui, D.; Chen, Y.; Liang, J., A Hierarchical Silver-Nanowire-Graphene Host Enabling Ultrahigh Rates and Superior Long-Term Cycling of Lithium-Metal Composite Anodes. *Adv. Mater.* **2018,** *30* (44), 1804165.
43. Liu, S.; Wang, A.; Li, Q.; Wu, J.; Chiou, K.; Huang, J.; Luo, J., Crumpled Graphene Balls Stabilized Dendrite-Free Lithium Metal Anodes. *Joule* **2018,** *2* (1), 184-193.
44. Yang, T.; Li, L.; Wu, F.; Chen, R., A Soft Lithiophilic Graphene Aerogel for Stable Lithium Metal Anode. *Adv. Funct. Mater.* **2020,** *30* (30), 2002013.
45. Li, N.; Zhang, K.; Xie, K.; Wei, W.; Gao, Y.; Bai, M.; Gao, Y.; Hou, Q.; Shen, C.; Xia, Z.; Wei, B., Reduced-Graphene-Oxide-Guided Directional Growth of Planar Lithium Layers. *Adv. Mater.* **2020,** *32* (7), 1907079.
46. Huang, G.; Han, J.; Zhang, F.; Wang, Z.; Kashani, H.; Watanabe, K.; Chen, M., Lithiophilic 3D Nanoporous Nitrogen-Doped Graphene for Dendrite-Free and Ultrahigh-Rate Lithium-Metal Anodes. *Adv. Mater.* **2019,** *31* (2), 1805334.
47. Zhou, Y.; Zhang, X.; Ding, Y.; Zhang, L.; Yu, G., Reversible Deposition of Lithium Particles Enabled by Ultraconformal and Stretchable Graphene Film for Lithium Metal Batteries. *Adv. Mater.* **2020,** *32* (48), 2005763.
48. Lu, L. L.; Ge, J.; Yang, J. N.; Chen, S. M.; Yao, H. B.; Zhou, F.; Yu, S. H., Free-Standing Copper Nanowire Network Current Collector for Improving Lithium Anode Performance. *Nano Lett.* **2016,** *16* (7), 4431-7.
49. Zhao, X.; Xia, S.; Zhang, X.; Pang, Y.; Xu, F.; Yang, J.; Sun, L.; Zheng, S., Highly Lithiophilic Copper-Reinforced Scaffold Enables Stable Li Metal Anode. *ACS Appl. Mater. Interfaces* **2021,** *13* (17), 20240-20250.
50. Zhang, C.; Lyu, R.; Lv, W.; Li, H.; Jiang, W.; Li, J.; Gu, S.; Zhou, G.; Huang, Z.; Zhang, Y.; Wu, J.; Yang, Q. H.; Kang, F., A Lightweight 3D Cu Nanowire Network with Phosphidation Gradient as Current Collector for High-Density Nucleation and Stable Deposition of Lithium. *Adv. Mater.* **2019,** *31* (48), 1904991.
51. Zhu, Z.-W.; Wang, Z.-Y.; Liu, S.; Li, G.-R.; Gao, X.-P., Uniform Lithium Plating within 3D Cu Foam Enabled by Ag Nanoparticles. *Electrochim. Acta* **2021,** *379*, 138152.
52. Yun, Q.; He, Y. B.; Lv, W.; Zhao, Y.; Li, B.; Kang, F.; Yang, Q. H., Chemical Dealloying Derived 3D Porous Current Collector for Li Metal Anodes. *Adv. Mater.* **2016,** *28* (32), 6932-9.
53. Li, Q.; Zhu, S. P.; Lu, Y. Y., 3D Porous Cu Current Collector/Li-Metal Composite Anode for Stable Lithium-Metal Batteries. *Adv. Funct. Mater.* **2017,** *27* (18), 1606422
54. Ke, X.; Cheng, Y.; Liu, J.; Liu, L.; Wang, N.; Liu, J.; Zhi, C.; Shi, Z.; Guo, Z., Hierarchically Bicontinuous Porous Copper as Advanced 3D Skeleton for Stable Lithium Storage. *ACS Appl.*

Mater. Interfaces **2018,** *10* (16), 13552-13561.
55. Wang, S. H.; Yin, Y. X.; Zuo, T. T.; Dong, W.; Li, J. Y.; Shi, J. L.; Zhang, C. H.; Li, N. W.; Li, C. J.; Guo, Y. G., Stable Li Metal Anodes *via* Regulating Lithium Plating/Stripping in Vertically Aligned Microchannels. *Adv. Mater.* **2017,** *29* (40), 1703729.
56. Huang, Z.; Zhang, C.; Lv, W.; Zhou, G.; Zhang, Y.; Deng, Y.; Wu, H.; Kang, F.; Yang, Q.-H., Realizing Stable Lithium Deposition by *in Situ* Grown Cu_2S Nanowires inside Commercial Cu Foam for Lithium Metal Anodes. *J. Mater. Chem. A* **2019,** *7* (2), 727-732.
57. Yang, C. P.; Yin, Y. X.; Zhang, S. F.; Li, N. W.; Guo, Y. G., Accommodating Lithium into 3D Current Collectors with a Submicron Skeleton towards Long-Life Lithium Metal Anodes. *Nat. Commun.* **2015,** *6*, 8058.
58. Wu, S.; Jiao, T.; Yang, S.; Liu, B.; Zhang, W.; Zhang, K., Lithiophilicity Conversion of the Cu Surface through Facile Thermal Oxidation: Boosting a Stable Li–Cu Composite Anode Through Melt Infusion. *J. Mater. Chem. A* **2019,** *7* (10), 5726-5732.
59. Chi, S.-S.; Liu, Y.; Song, W.-L.; Fan, L.-Z.; Zhang, Q., Prestoring Lithium into Stable 3D Nickel Foam Host as Dendrite-Free Lithium Metal Anode. *Adv. Funct. Mater.* **2017,** *27* (24).
60. Yu, L.; Canfield, N. L.; Chen, S.; Lee, H.; Ren, X.; Engelhard, M. H.; Li, Q.; Liu, J.; Xu, W.; Zhang, J. G., Enhanced Stability of Lithium Metal Anode by Using a 3D Porous Nickel Substrate. *ChemElectroChem* **2018,** *5* (5), 761-769.
61. Huang, X.; Feng, X.; Zhang, B.; Zhang, L.; Zhang, S.; Gao, B.; Chu, P. K.; Huo, K., Lithiated $NiCo_2O_4$ Nanorods Anchored on 3D Nickel Foam Enable Homogeneous Li Plating/Stripping for High-Power Dendrite-Free Lithium Metal Anode. *ACS Appl. Mater. Interfaces* **2019,** *11* (35), 31824-31831.
62. Huang, G.; Guo, P.; Wang, J.; Chen, S.; Liang, J.; Tao, R.; Tang, S.; Zhang, X.; Cheng, S.; Cao, Y.-C.; Dai, S., Lithiophilic V_2O_5 Nanobelt Arrays Decorated 3D Framework Hosts for Highly Stable Composite Lithium Metal Anodes. *Chem. Eng. J.* **2020,** *384*, 123313.
63. Zhao, F.; Zhou, X.; Deng, W.; Liu, Z., Entrapping Lithium Deposition in Lithiophilic Reservoir Constructed by Vertically Aligned ZnO Nanosheets for Dendrite-Free Li Metal Anodes. *Nano Energy* **2019,** *62*, 55-63.
64. Jiang, H.; Fan, H.; Han, Z.; Hong, B.; Wu, F.; Zhang, K.; Zhang, Z.; Fang, J.; Lai, Y., A 3D Conducting Scaffold with *in-Situ* Grown Lithiophilic Ni_2P Nanoarrays for High Stability Lithium Metal Anodes. *J. Energy Chem.* **2021,** *54*, 301-309.
65. Zhu, J.; Chen, J.; Luo, Y.; Sun, S.; Qin, L.; Xu, H.; Zhang, P.; Zhang, W.; Tian, W.; Sun, Z., Lithiophilic Metallic Nitrides Modified Nickel Foam by Plasma for Stable Lithium Metal Anode. *Energy Storage Mater.* **2019,** *23*, 539-546.
66. Zhang, Z.; Wang, J.; Yan, X.; Zhang, S.; Yang, W.; Zhuang, Z.; Han, W.-Q., *In-Situ* Growth of Hierarchical *N*-Doped CNTs/Ni Foam Scaffold for Dendrite-Free Lithium Metal Anode. *Energy Storage Mater.* **2020,** *29*, 332-340.
67. Jin, J.; Cai, W.; Cai, J.; Shao, Y.; Song, Y.; Xia, Z.; Zhang, Q.; Sun, J., MOF-Derived Hierarchical CoP Nanoflakes Anchored on Vertically Erected Graphene Scaffolds as Self-Supported and Flexible Hosts for Lithium–Sulfur Batteries. *J. Mater. Chem. A* **2020,** *8* (6), 3027-3034.
68. Ci, H.; Cai, J.; Ma, H.; Shi, Z.; Cui, G.; Wang, M.; Jin, J.; Wei, N.; Lu, C.; Zhao, W.; Sun, J.; Liu, Z., Defective VSe_2-Graphene Heterostructures Enabling *in Situ* Electrocatalyst Evolution for Lithium-Sulfur Batteries. *ACS Nano* **2020,** *14* (9), 11929-11938.

69. Lei, T.; Chen, W.; Huang, J.; Yan, C.; Sun, H.; Wang, C.; Zhang, W.; Li, Y.; Xiong, J., Multi-Functional Layered WS_2 Nanosheets for Enhancing the Performance of Lithium-Sulfur Batteries. *Adv. Energy Mater.* **2017,** *7* (4), 1601843.
70. Xu, J.; Yang, L.; Cao, S.; Wang, J.; Ma, Y.; Zhang, J.; Lu, X., Sandwiched Cathodes Assembled from CoS_2-Modified Carbon Clothes for High-Performance Lithium-Sulfur Batteries. *Adv. Sci. (Weinh)* **2021**, 2101019.
71. Wang, J.; Zhao, Y.; Li, G.; Luo, D.; Liu, J.; Zhang, Y.; Wang, X.; Shui, L.; Chen, Z., Aligned Sulfur-Deficient ZnS_{1-x} Nanotube Arrays as Efficient Catalyzer for High-Performance Lithium/Sulfur Batteries. *Nano Energy* **2021,** *84*, 105891.
72. Wang, Z.; Shen, J.; Liu, J.; Xu, X.; Liu, Z.; Hu, R.; Yang, L.; Feng, Y.; Liu, J.; Shi, Z.; Ouyang, L.; Yu, Y.; Zhu, M., Self-Supported and Flexible Sulfur Cathode Enabled *via* Synergistic Confinement for High-Energy-Density Lithium-Sulfur Batteries. *Adv. Mater.* **2019,** *31* (33), 1902228.
73. Wang, M.; Fan, L.; Tian, D.; Wu, X.; Qiu, Y.; Zhao, C.; Guan, B.; Wang, Y.; Zhang, N.; Sun, K., Rational Design of Hierarchical SnO_2/1T-MoS_2 Nanoarray Electrode for Ultralong-Life Li–S Batteries. *ACS Energy Lett.* **2018,** *3* (7), 1627-1633.
74. Zhong, Y.; Chao, D.; Deng, S.; Zhan, J.; Fang, R.; Xia, Y.; Wang, Y.; Wang, X.; Xia, X.; Tu, J., Confining Sulfur in Integrated Composite Scaffold with Highly Porous Carbon Fibers/Vanadium Nitride Arrays for High-Performance Lithium-Sulfur Batteries. *Adv. Funct. Mater.* **2018,** *28* (38), 1706391.
75. Yuan, Z.; Peng, H.-J.; Huang, J.-Q.; Liu, X.-Y.; Wang, D.-W.; Cheng, X.-B.; Zhang, Q., Hierarchical Free-Standing Carbon-Nanotube Paper Electrodes with Ultrahigh Sulfur-Loading for Lithium-Sulfur Batteries. *Adv. Funct. Mater.* **2014,** *24* (39), 6105-6112.
76. Jin, S.; Xin, S.; Wang, L.; Du, Z.; Cao, L.; Chen, J.; Kong, X.; Gong, M.; Lu, J.; Zhu, Y.; Ji, H.; Ruoff, R. S., Covalently Connected Carbon Nanostructures for Current Collectors in Both the Cathode and Anode of Li-S Batteries. *Adv. Mater.* **2016,** *28* (41), 9094-9102.
77. Mao, Y.; Li, G.; Guo, Y.; Li, Z.; Liang, C.; Peng, X.; Lin, Z., Foldable Interpenetrated Metal-Organic Frameworks/Carbon Nanotubes Thin Film for Lithium-Sulfur Batteries. *Nat. Commun.* **2017,** *8*, 14628.
78. Zhang, Y.; Li, G.; Wang, J.; Luo, D.; Sun, Z.; Zhao, Y.; Yu, A.; Wang, X.; Chen, Z., "Sauna" Activation toward Intrinsic Lattice Deficiency in Carbon Nanotube Microspheres for High-Energy and Long-Lasting Lithium–Sulfur Batteries. *Adv. Energy Mater.* **2021**, 2100497.
79. Xin, S.; Gu, L.; Zhao, N. H.; Yin, Y. X.; Zhou, L. J.; Guo, Y. G.; Wan, L. J., Smaller Sulfur Molecules Promise Better Lithium-Sulfur Batteries. *J. Am. Chem. Soc.* **2012,** *134* (45), 18510-18513.
80. Chen, T.; Zhang, Z.; Cheng, B.; Chen, R.; Hu, Y.; Ma, L.; Zhu, G.; Liu, J.; Jin, Z., Self-Templated Formation of Interlaced Carbon Nanotubes Threaded Hollow Co_3S_4 Nanoboxes for High-Rate and Heat-Resistant Lithium-Sulfur Batteries. *J. Am. Chem. Soc.* **2017,** *139* (36), 12710-12715.
81. Zhong, Y.; Yin, L.; He, P.; Liu, W.; Wu, Z.; Wang, H., Surface Chemistry in Cobalt Phosphide-Stabilized Lithium-Sulfur Batteries. *J. Am. Chem. Soc.* **2018,** *140* (4), 1455-1459.
82. Gueon, D.; Hwang, J. T.; Yang, S. B.; Cho, E.; Sohn, K.; Yang, D. K.; Moon, J. H., Spherical Macroporous Carbon Nanotube Particles with Ultrahigh Sulfur Loading for Lithium-Sulfur Battery Cathodes. *ACS Nano* **2018,** *12* (1), 226-233.
83. Pan, H.; Cheng, Z.; Chen, J.; Wang, R.; Li, X., High Sulfur Content and Volumetric Capacity

Promised by a Compact Freestanding Cathode for High-Performance Lithium–Sulfur Batteries. *Energy Storage Mater.* **2020,** *27*, 435-442.
84. Li, G.; Lei, W.; Luo, D.; Deng, Y.; Deng, Z.; Wang, D.; Yu, A.; Chen, Z., Stringed "Tube on Cube" Nanohybrids as Compact Cathode Matrix for High-Loading and Lean-Electrolyte Lithium–Sulfur Batteries. *Energy Environ. Sci.* **2018,** *11* (9), 2372-2381.
85. Kang, W.; Fan, L.; Deng, N.; Zhao, H.; Li, Q.; Naebe, M.; Yan, J.; Cheng, B., Sulfur-Embedded Porous Carbon Nanofiber Composites for High Stability Lithium-Sulfur Batteries. *Chem. Eng. J.* **2018,** *333*, 185-190.
86. Lee, J. S.; Kim, W.; Jang, J.; Manthiram, A., Sulfur-Embedded Activated Multichannel Carbon Nanofiber Composites for Long-Life, High-Rate Lithium-Sulfur Batteries. *Adv. Energy Mater.* **2017,** *7* (5), 1601943.
87. Lee, J. S.; Jun, J.; Jang, J.; Manthiram, A., Sulfur-Immobilized, Activated Porous Carbon Nanotube Composite Based Cathodes for Lithium-Sulfur Batteries. *Small* **2017,** *13* (12), 1602984.
88. Li, Z.; Zhang, J. T.; Chen, Y. M.; Li, J.; Lou, X. W., Pie-Like Electrode Design for High-Energy Density Lithium-Sulfur Batteries. *Nat. Commun.* **2015,** *6*, 8850.
89. Zhang, X.; Shang, C.; Akinoglu, E. M.; Wang, X.; Zhou, G., Constructing Co_3S_4 Nanosheets Coating *N*-Doped Carbon Nanofibers as Freestanding Sulfur Host for High-Performance Lithium–Sulfur Batteries. *Adv. Sci.* **2020**, *7* (22), 2002037.
90. Li, Z.; Guan, B. Y.; Zhang, J.; Lou, X. W., A Compact Nanoconfined Sulfur Cathode for High-Performance Lithium-Sulfur Batteries. *Joule* **2017,** *1* (3), 576-587.
91. Song, J.; Yu, Z.; Gordin, M. L.; Wang, D., Advanced Sulfur Cathode Enabled by Highly Crumpled Nitrogen-Doped Graphene Sheets for High-Energy-Density Lithium-Sulfur Batteries. *Nano Lett.* **2016,** *16* (2), 864-70.
92. Duan, L.; Zhao, L.; Cong, H.; Zhang, X.; Lü, W.; Xue, C., Plasma Treatment for Nitrogen-Doped 3D Graphene Framework by a Conductive Matrix with Sulfur for High-Performance Li-S Batteries. *Small* **2019,** *15* (7), 1804347.
93. Gómez-Urbano, J. L.; Gómez-Cámer, J. L.; Botas, C.; Díez, N.; López del Amo, J. M.; Rodríguez-Martinez, L. M.; Carriazo, D.; Rojo, T., Hydrothermally Reduced Graphene Oxide for the Effective Wrapping of Sulfur Particles Showing Long Term Stability as Electrodes for Li-S Batteries. *Carbon* **2018,** *139*, 226-233.
94. Wang, Y.; Huang, J.; Chen, X.; Wang, L.; Ye, Z., Powder Metallurgy Template Growth of 3D *N*-Doped Graphene Foam as Binder-Free Cathode for High-Performance Lithium/Sulfur Battery. *Carbon* **2018,** *137*, 368-378.
95. Li, B.; Xiao, Q.; Luo, Y., A Modified Synthesis Process of Three-Dimensional Sulfur/Graphene Aerogel as Binder-Free Cathode for Lithium-Sulfur Batteries. *Mater. Des.* **2018,** *153*, 9-14.
96. Huang, J.-Q.; Liu, X.-F.; Zhang, Q.; Chen, C.-M.; Zhao, M.-Q.; Zhang, S.-M.; Zhu, W.; Qian, W.-Z.; Wei, F., Entrapment of Sulfur in Hierarchical Porous Graphene for Lithium–Sulfur Batteries with High Rate Performance from −40 to 60°C. *Nano Energy* **2013,** *2* (2), 314-321.
97. Xu, J.; Su, D.; Zhang, W.; Bao, W.; Wang, G., A Nitrogen–Sulfur co-Doped Porous Graphene Matrix as a Sulfur Immobilizer for High Performance Lithium–Sulfur Batteries. *J. Mater. Chem. A* **2016,** *4* (44), 17381-17393.
98. Cao, J.; Chen, C.; Zhao, Q.; Zhang, N.; Lu, Q.; Wang, X.; Niu, Z.; Chen, J., A Flexible Nanostructured Paper of a Reduced Graphene Oxide-Sulfur Composite for High-Performance

Lithium-Sulfur Batteries with Unconventional Configurations. *Adv. Mater.* **2016,** *28* (43), 9629-9636.